Non-symmetric pillar[5]arene based on triazole-linked 8-oxyquinolines as a sequential sensor for thorium(IV) followed by fluoride ion

Yuyu Fang, Caixia Li, Lei Wu, Bing Bai, Xing Li, Yiming Jia, Wen Feng* and Lihua Yuan*

Institute of Nuclear Science and Technology, Key Laboratory for Radiation Physics and Technology of Ministry of Education, College of Chemistry, Sichuan University, Chengdu 610064, China. Fax: +86-28-85418755; Tel: +86-28-85412890; E-mail: wfeng9510@scu.edu.cn; lhyuan@scu.edu.cn

Supporting Information

Contents

1. General information

The ^{1}H NMR and ^{13}C NMR spectra were recorded on Bruker AVANCE AV II-400 MHz (^{1}H: 400 MHz; ^{13}C: 100 MHz). Chemical shifts are reported in δ values in ppm using tetramethlysilane (TMS) and coupling constants (J) are denoted in Hz. Multiplicities are denoted as follows: s = singlet, d = doublet, t = triplet, dd = double doublet and m = multiplet. High resolution mass (HRMS) data were obtained by WATERS Q-TOF Premier. Solvents for extraction and chromatography were reagent grade. CH_2Cl_2 was distilled from CaH_2. $CDCl_3$ and acetone-d_6 were from Cambridge Isotope Laboratories (CIL). All chemicals were obtained from commercial suppliers and were used as received unless otherwise noted. Fluorescence emission spectra were obtained using FluoroMax-4 Spectrofluorophotometer (HORIBA Jobin Yvon). UV-vis absorption spectra were recorded on SHIMADZU UV-2450.

2. Synthesis and characterization

Synthetic route

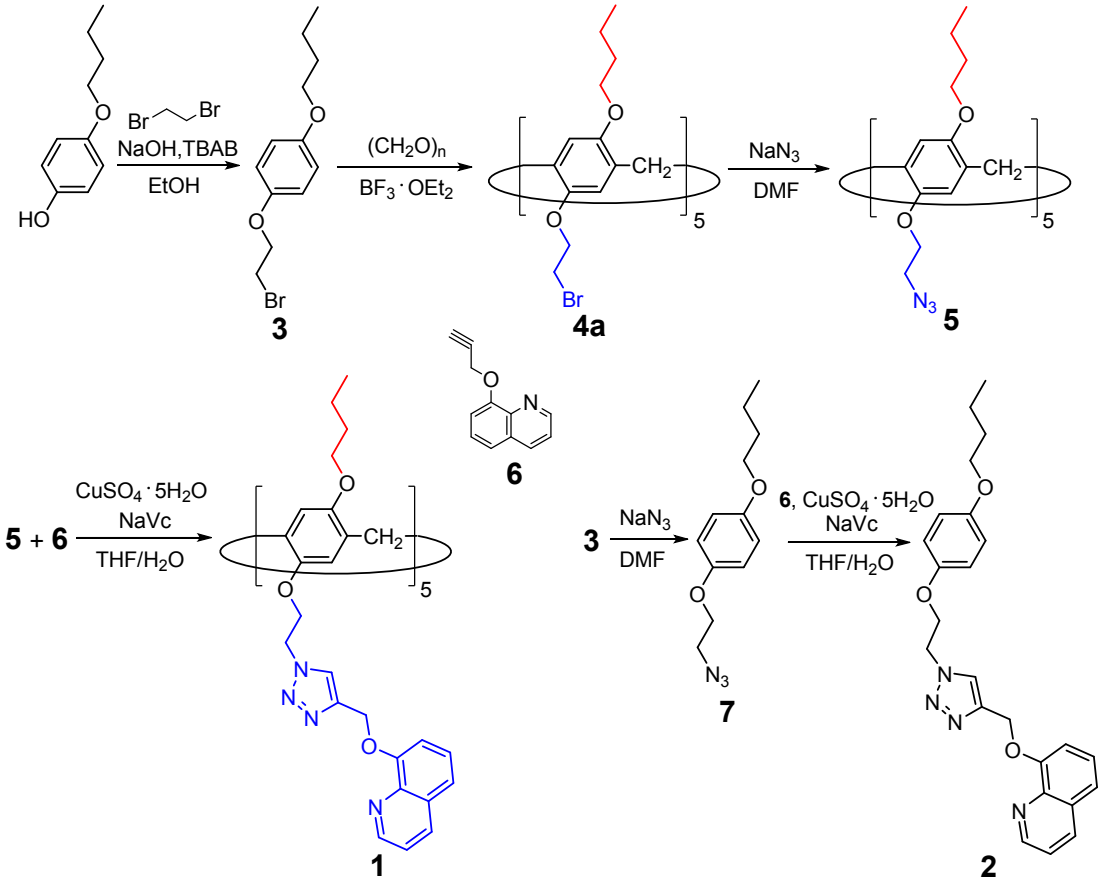

Scheme S1 Synthesis of non-symmetric pillar[5]arene **1** and its model compound of noncyclic monomeric analog **2**.

Synthesis of compound 3

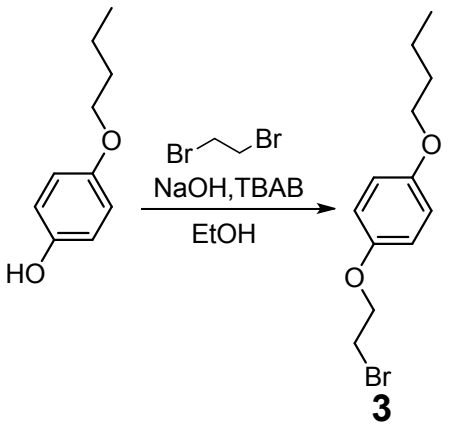

1,2-dibromoethane (12.4 g, 66.2 mmol) and the phase-transfer catalyst tetrabutyl ammonium bromide (TBAB) (1.94 g, 6.02 mmol) were added to a solution of 4-butoxyphenol[S1] (10.0 g, 60.2 mmol) and NaOH (2.65 g, 66.2 mmol) in ethanol (250 mL) under nitrogen atmosphere. The solution was refluxed for 24 h. After removal of the inorganic salt, the solvent was removed under reduced pressure and the residue was recrystallized by petroleum ether to afford the crude product which was further purified by silica gel column chromatography using petroleum ether/dichloromethane (1:1, v/v) as the eluent to give **3** (6.57 g, 40%) as a white solid. ^{1}H NMR (400 MHz, $CDCl_3$) δ 6.84 (m, 4 H), 4.24 (t, J = 6.3 Hz, 2 H), 3.91 (t, J = 6.5 Hz, 2 H), 3.61 (t, J = 6.3 Hz, 2 H), 1.74 (m, 2 H), 1.48 (m, 2 H), 0.97 (m, J = 7.4 Hz, 2 H). ^{13}C NMR (100 MHz, $CDCl_3$) δ 153.97, 152.07, 116.05, 115.45, 68.80, 68.28, 31.44, 29.42, 19.28, 13.91.

Synthesis of compound 4a

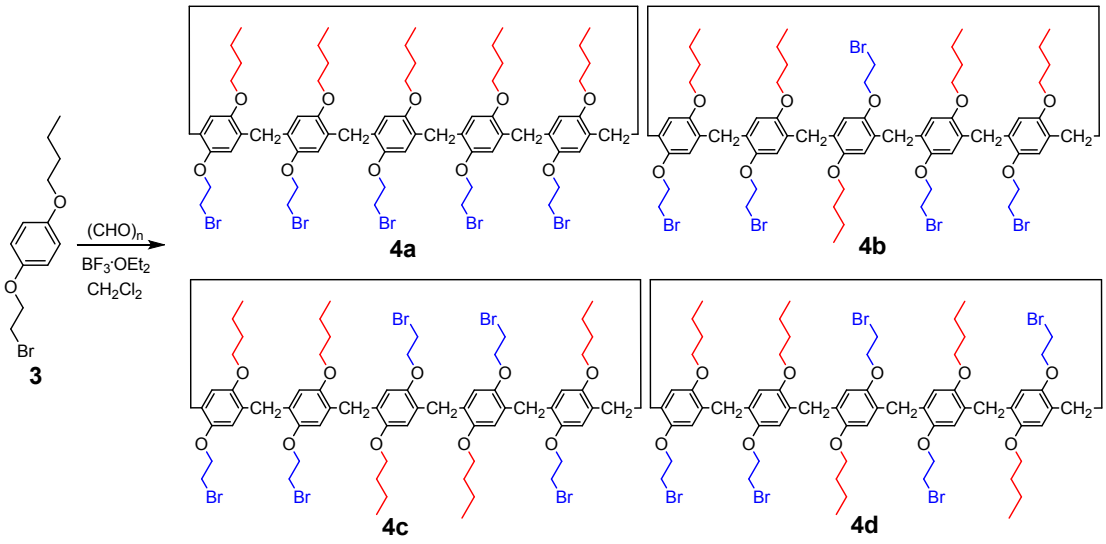

To a solution of **3** (10.0 g, 36.6 mmol) in dry dichloromethane (250 mL) was added paraformaldehyde (1.12 g, 37.0 mmol) under nitrogen atmosphere. Then boron trifluoride diethyl etherate (5.72 g, 40.3 mmol) was added to the solution and the mixture was stirred at room temperature for 2 h. Water (100 mL) was added to quench the reaction. The organic layer was washed twice with H_2O (2 × 100 mL) and dried over anhydrous Na_2SO_4. The solvent was removed under reduced pressure to afford

the crude product. The obtained solid was purified by column chromatography on silica gel with petroleum ether/dichloromethane (1:1, v/v) as the eluent to afford **4** as a white powder. Pillar[5]arene **4** has four constitutional isomers **4a**, **4b**, **4c**, and **4d**. The structure of **4a** could be easily determined since its proton NMR spectrum was analyzable[S2] and it was separated lastly. The proton NMR spectrum of **4a** (520 mg, 5.0%) is shown in Fig. S3. ^{1}H NMR (400 MHz, $CDCl_3$) δ 6.90 (s, 5 H), 6.80 (s, 5 H), 4.17 (t, J = 5.7 Hz, 10 H), 3.87 (t, J = 6.5 Hz, 10 H), 3.80 (s, 10 H), 3.59 (t, J = 5.7 Hz, 10 H), 1.79 (m, 10 H), 1.51 (m, 10 H), 098 (t, J = 7.4 Hz, 15 H). ^{13}C NMR (100 MHz, $CDCl_3$) δ 150.62, 148.94, 128.93, 128.41, 116.29, 114.73, 69.07, 68.01, 31.98, 30.79, 29.47, 19.54, 14.05. ESI-HRMS (m/z) calcd for $C_{65}H_{85}O_{10}Br_5$ $[M + Na]^+$ 1449.1896, $[M + K]^+$ 1465.1635; found $[M + Na]^+$ 1449.1908, $[M + K]^+$ 1465.1649.

Synthesis of compound 5

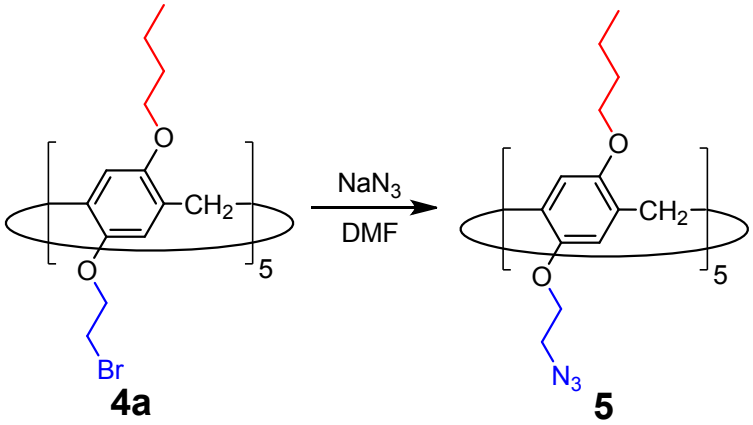

4a **5**

To a solution of **4a** (1.00 g, 0.70 mmol) in dry DMF (80 mL) was added sodium azide (365 mg, 5.61 mmol) under nitrogen atmosphere. The mixture was stirred at 90 °C for 12 h and cooled to room temperature. After slow addition of ice water to the solution, the precipitate was collected by filtration and washed with water (2 × 100 mL) and methanol (2 × 100 mL) to afford **5** as a white solid (850 mg, 98%).^{1}H NMR (400 MHz, $CDCl_3$) δ 6.85 (s, 5 H), 6.82 (s, 5 H), 4.00 (t, J = 5.7 Hz, 10 H), 3.86 (t, J = 6.5 Hz, 10 H), 3.79 (s, 10 H), 3.55 (t, J = 5.7 Hz, 10 H), 1.78 (m, 10 H), 1.51 (m, 10 H), 098 (t, J = 7.4 Hz, 15 H). ^{13}C NMR (100 MHz, $CDCl_3$) δ 150.65, 149.11, 128.72, 128.45, 115.55, 115.05, 68.15, 67.42, 51.10, 31.96, 29.55, 19.52, 14.03. ESI-HRMS

(m/z) calcd for $C_{65}H_{85}N_{15}O_{10}$ $[M + Na]^+$ 1258.6502, $[M + K]^+$ 1274.6241; found $[M + Na]^+$ 1258.6504, $[M + K]^+$ 1274.6270.

Synthesis of compound 1

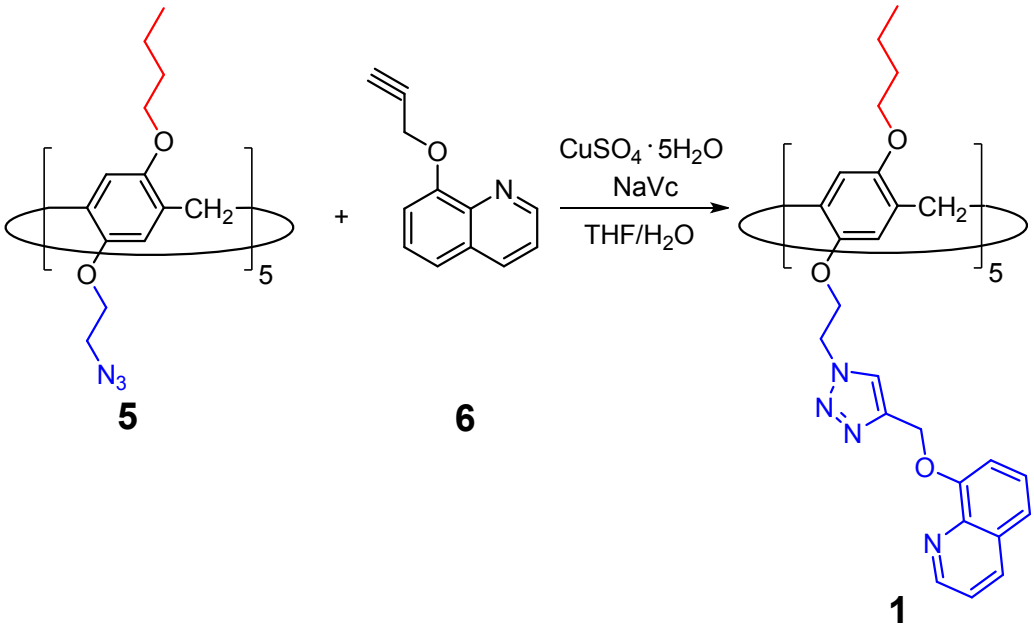

$CuSO_4$•$5H_2O$ (6.10 mg, 0.024 mmol) and sodium ascorbate (24.1 mg, 0.121 mmol) were added to a mixed solution consisting of **5** (300 mg, 0.243 mmol) and 8-propynoxyquinoline **6**[S3] (245 mg, 1.34 mmol) in THF/H_2O (4:1, v/v) (100 mL) under nitrogen atmosphere. The resulting mixture was stirred at 60 °C for 12 h. After removal of the solvent under reduced pressure, the residue was dissolved in CH_2Cl_2 and washed with H_2O (2 × 100 mL) and 5% NH_3•H_2O (2 × 100 mL). The organic layer was dried over anhydrous $NaSO_4$ and concentrated. The obtained crude product was purified by column chromatography on neutral aluminium oxide (eluent: CH_2Cl_2/CH_3OH = 100:1, v/v) to afford the desired product **1** (365 mg, yield 72%). ^{1}H NMR (400 MHz, $CDCl_3$) δ 8.83 (dd, 5 H), 8.01 (dd, 5 H), 7.93 (s, 5 H), 7.30 (m, 20 H), 6.63 (s, 5 H), 6.48 (s, 5 H), 5.47 (s, 10 H), 4.55 (m, 10 H), 4.03 (d, J = 1.5 Hz, 10 H), 3.76 (t, J = 6.2 Hz, 10 H), 3.36 (s, 10 H), 1.71 (m, 10 H), 1.49 (m, 10 H), 0.95 (t, J = 7.4 Hz, 15 H). ^{13}C NMR (100 MHz, $CDCl_3$) δ 153.77, 150.59, 149.16, 148.62, 143.97, 140.17, 135.84, 129.37, 128.74, 128.29, 126.65, 124.04, 121.53, 120.08, 116.11, 114.64, 109.89, 67.99, 67.39, 62.68, 50.31, 31.86, 29.56, 19.46, 14.02. ESI-

HRMS (m/z) calcd for $C_{125}H_{130}N_{20}O_{15}$ $[M + H]^+$ 2152.0103, $[M + Na]^+$ 2174.9956; found $[M + H]^+$ 2152.0127, $[M + Na]^+$ 2174.9961.

Synthesis of compound 2

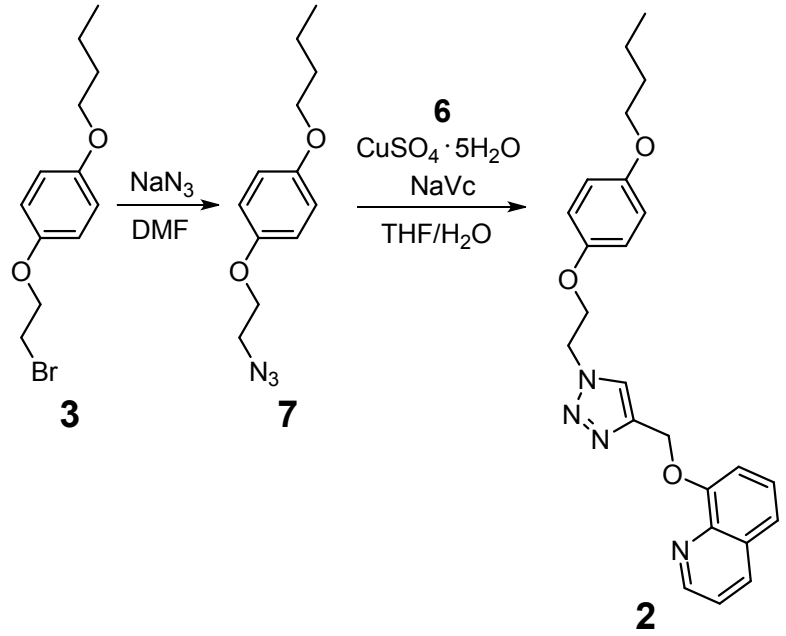

A mixture of **3** (1.00 g, 3.66 mmol) and sodium azide (476 mg, 7.32 mmol) in dry DMF (10 mL) was stirred at 90 °C under nitrogen atmosphere for 6 h. After removal of the solvent under reduced pressure, the residue was dissolved in CH_2Cl_2 and washed with H_2O (2 × 100 mL). The organic layer was dried over anhydrous $NaSO_4$ and concentrated to afford **7** as white oil which was used without further purification. The resulting oil **7** was dissolved together with 8-propynoxyquinoline **6** (805 mg, 4.39 mmol), $CuSO_4$•$5H_2O$ (9.20 mg, 0.037 mmol) and sodium ascorbate (14.5 mg, 0.073 mmol) in THF/H_2O (4:1, v/v) (100 mL) at 60 °C for 6 h under nitrogen atmosphere. After removal of the solvent under reduced pressure, the residue was dissolved in CH_2Cl_2 and washed with H_2O (2 × 100 mL) and 5% NH_3•H_2O (2 × 100 mL). The organic layer was dried over anhydrous $NaSO_4$ and concentrated. The obtained crude product was purified by column chromatography on silica gel (eluent: CH_2Cl_2/CH_3OH = 25:1, v/v) to afford the desired product **2** (1.20 g, yield 78%). ^{1}H NMR (400 MHz, $CDCl_3$) δ 8.94 (d, *J* = 2.8 Hz, 1 H), 8.13 (d, *J* = 7.4 Hz, 1 H), 7.95 (s, 1 H), 7.42 (m, 3 H), 7.33 (m, 1 H), 6.77 (d, *J* = 9.1 Hz, 2 H), 6.71 (d, *J* = 9.1 Hz,

2H), 5.59 (s, 2 H), 4.70 (t, J = 5.0 Hz, 2 H), 4.28 (t, J = 5.0 Hz, 2 H), 3.88 (t, J = 6.5 Hz, 2 H), 1.73 (m, 2 H), 1.47 (m, 2 H), 0.96 (t, J = 7.4 Hz, 3 H). ^{13}C NMR (100 MHz, $CDCl_3$) δ 153.96, 153.81, 151.70, 149.32, 144.06, 140.29, 135.96, 129.46, 126.73, 124.52, 121.63, 120.18, 115.61, 115.41, 109.94, 68.23, 66.94, 62.80, 49.86, 31.36, 19.22, 13.87. ESI-HRMS (m/z) calcd for $C_{24}H_{26}N_4O_3$ $[M + H]^+$ 419.2083, $[M + Na]^+$ 441.1903, $[M + K]^+$ 457.1642; found $[M + H]^+$ 419.2083, $[M + Na]^+$ 441.1909, $[M + K]^+$ 457.1647.

3. NMR and ESI-HRMS spectra

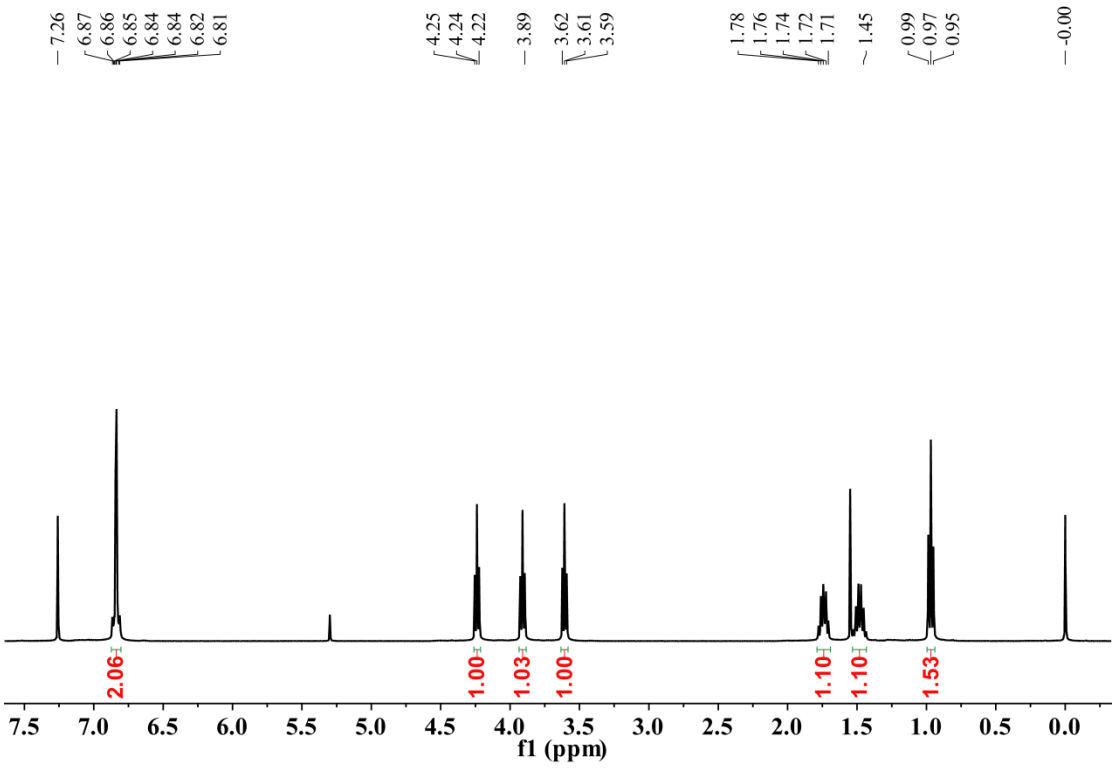

Fig. S1 ^{1}H NMR spectrum (400 MHz, $CDCl_3$) of **3** at 298 K.

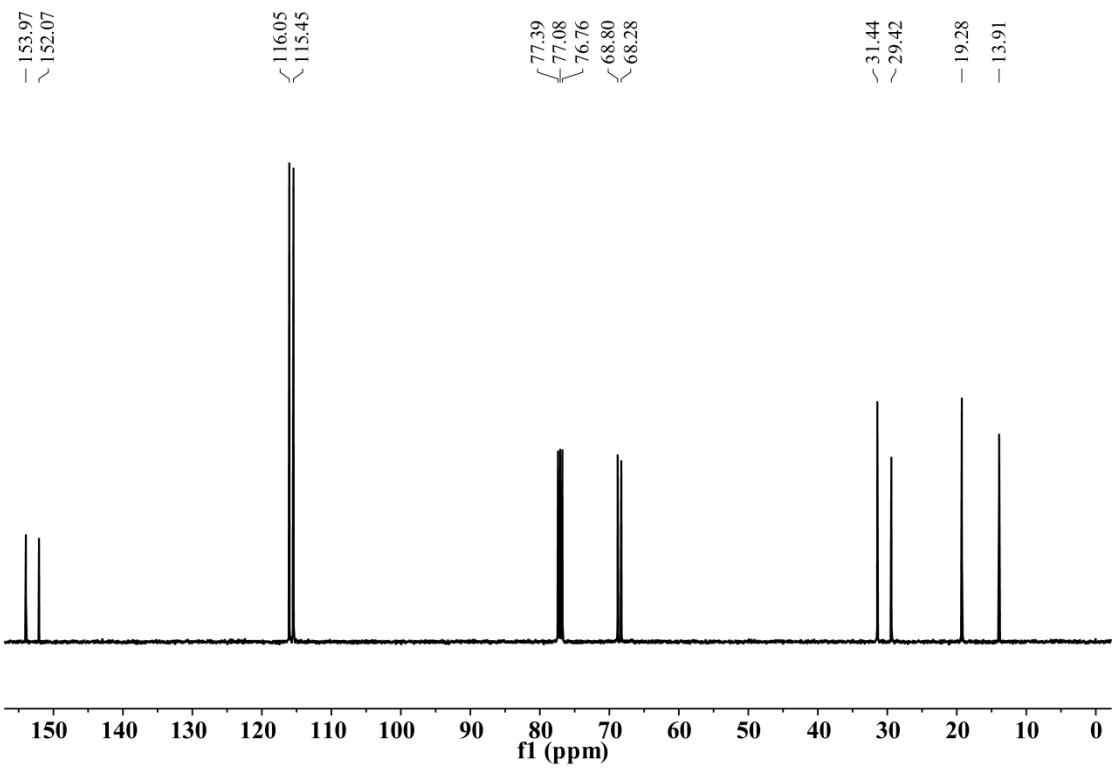

Fig. S2 ^{13}C NMR spectrum (100 MHz, $CDCl_3$) of **3** at 298 K.

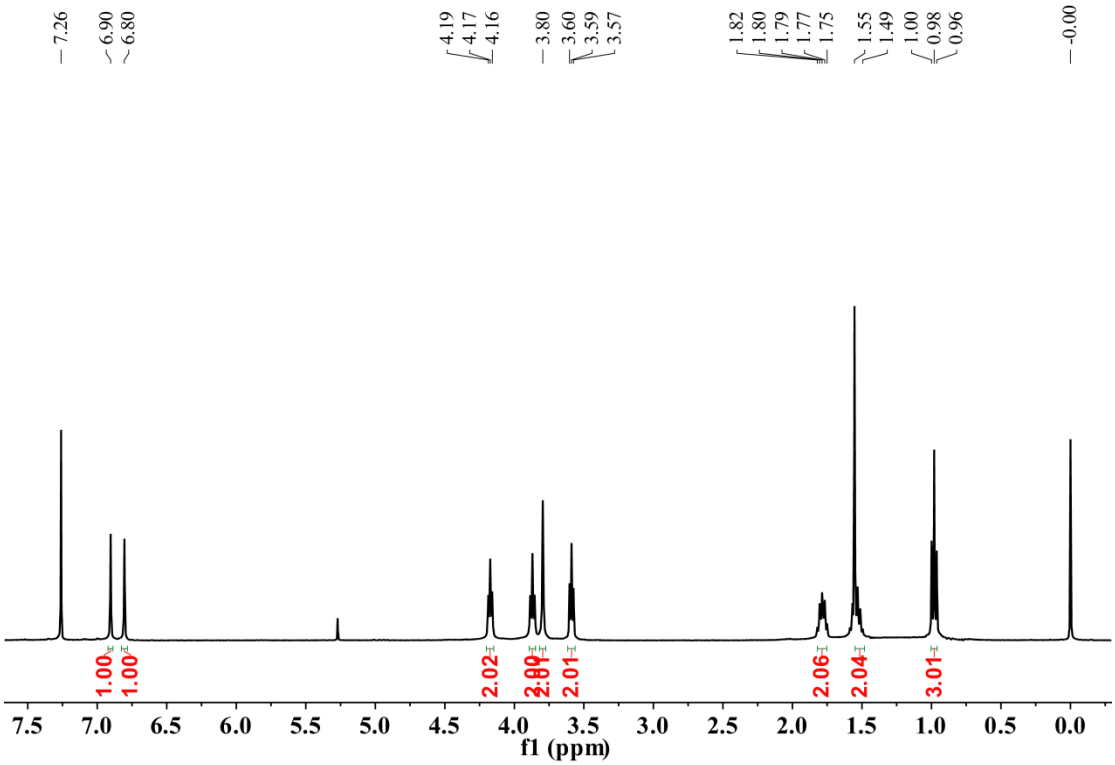

Fig. S3 ^{1}H NMR spectrum (400 MHz, $CDCl_3$) of **4a** at 298 K.

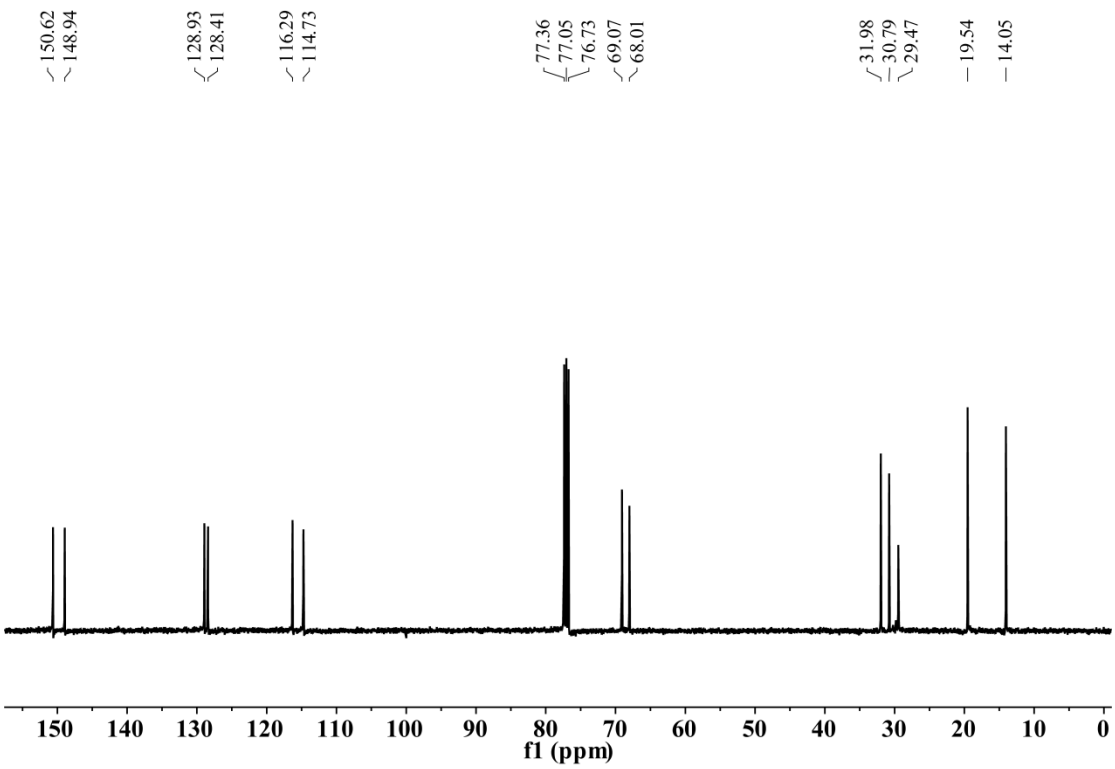

Fig. S4 ^{13}C NMR spectrum (100 MHz, $CDCl_3$) of **4a** at 298 K.

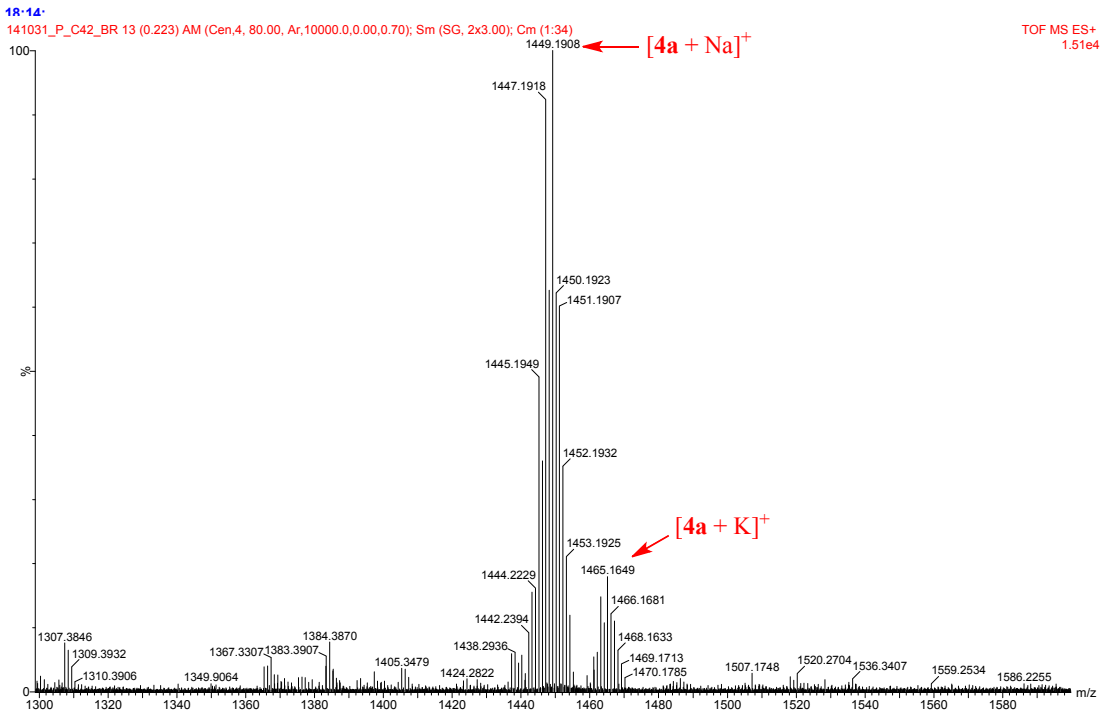

Fig. S5 ESI-HRMS spectrum of **4a**.

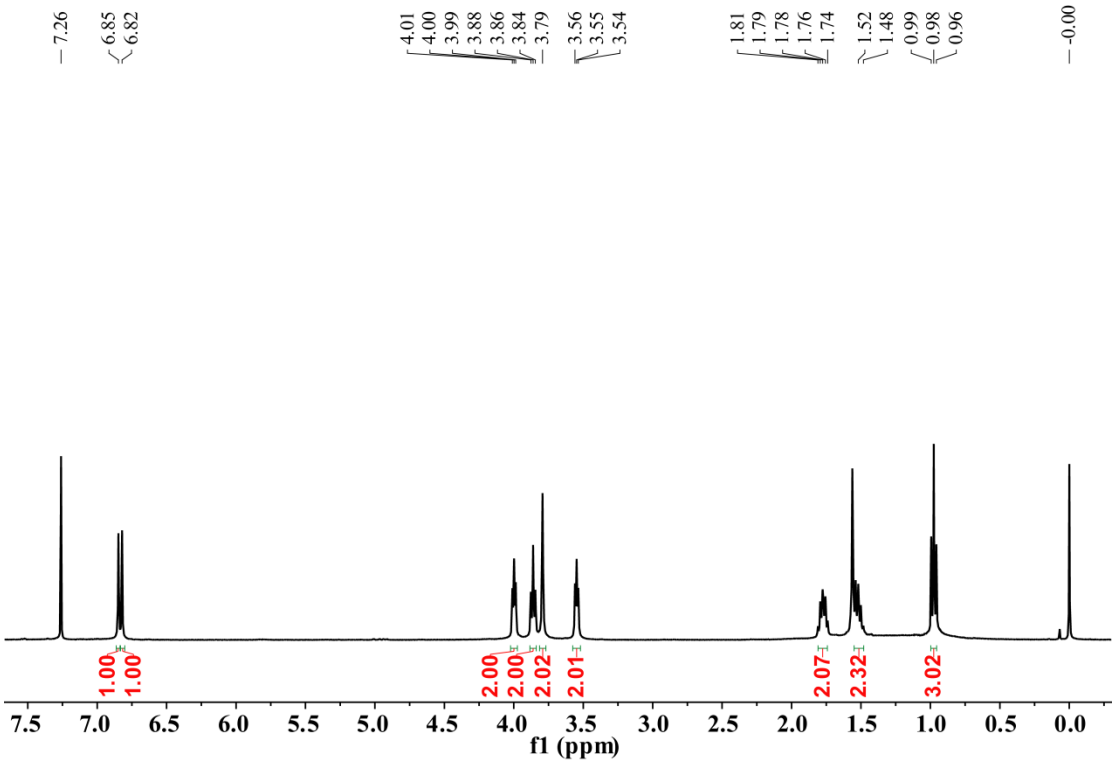

Fig. S6 ^{1}H NMR spectrum (400 MHz, $CDCl_3$) of **5** at 298 K.

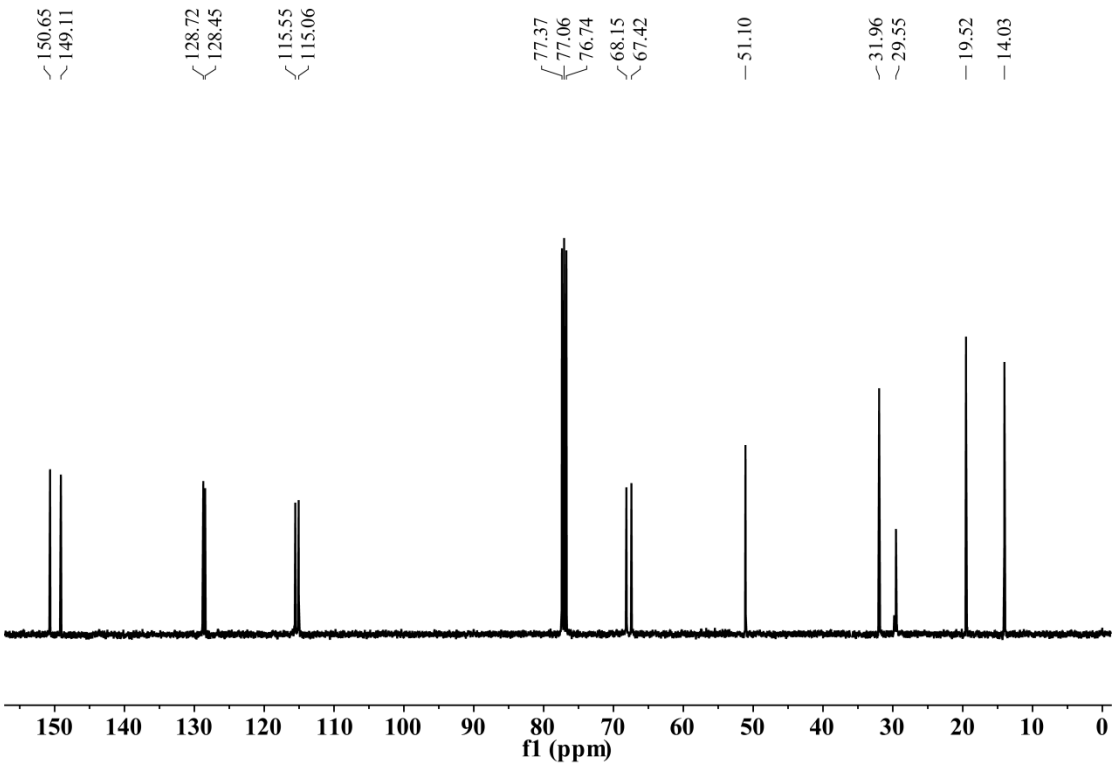

Fig. S7 ^{13}C NMR spectrum (100 MHz, $CDCl_3$) of **5** at 298 K.

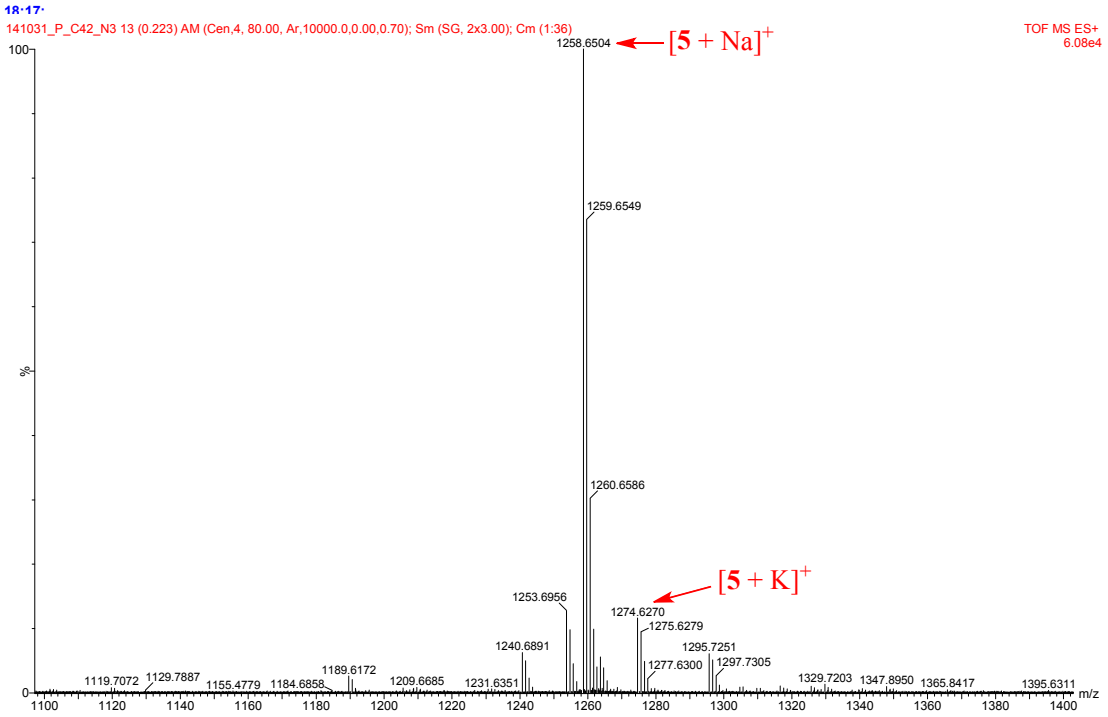

Fig. S8 ESI-HRMS spectrum of **5**.

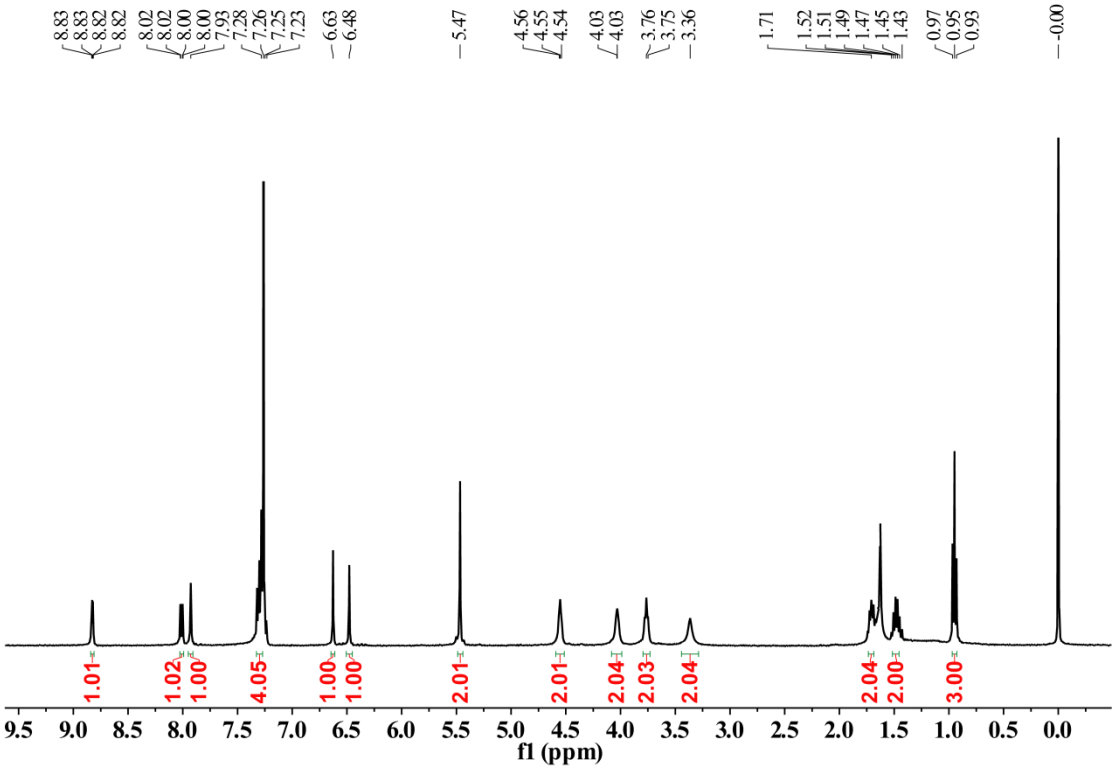

Fig. S9 ^{1}H NMR spectrum (400 MHz, $CDCl_3$) of **1** at 298 K.

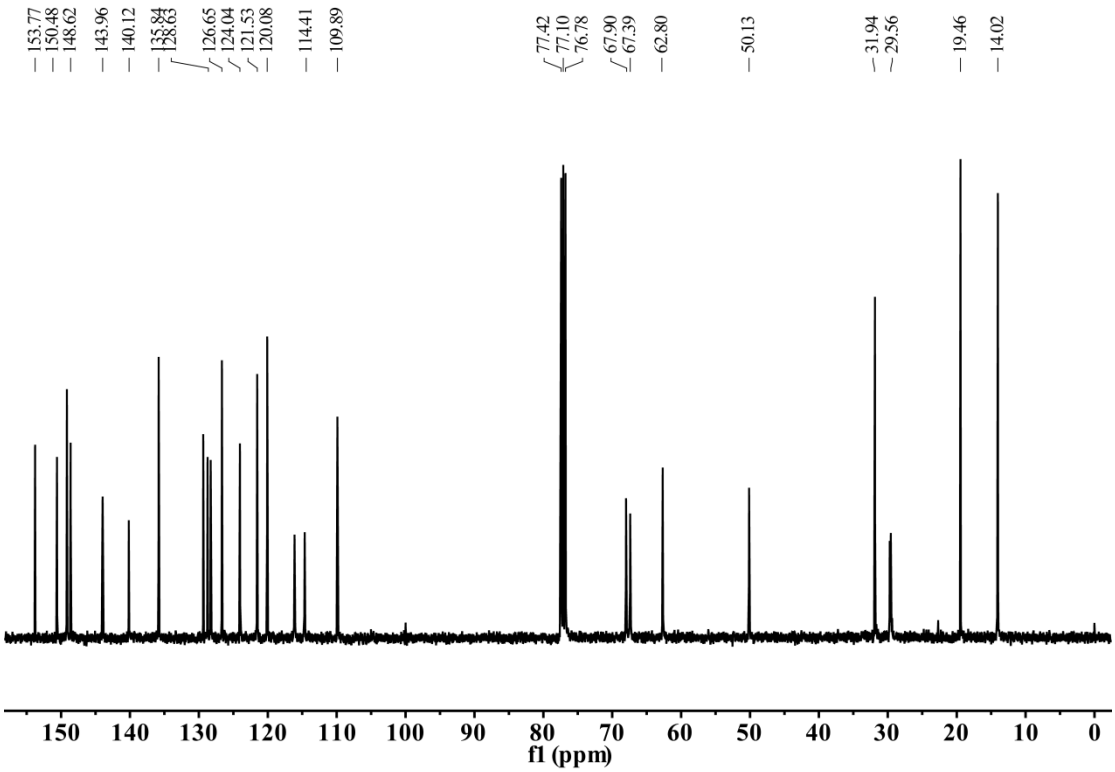

Fig. S10 ^{13}C NMR spectrum (100 MHz, $CDCl_3$) of **1** at 298 K.

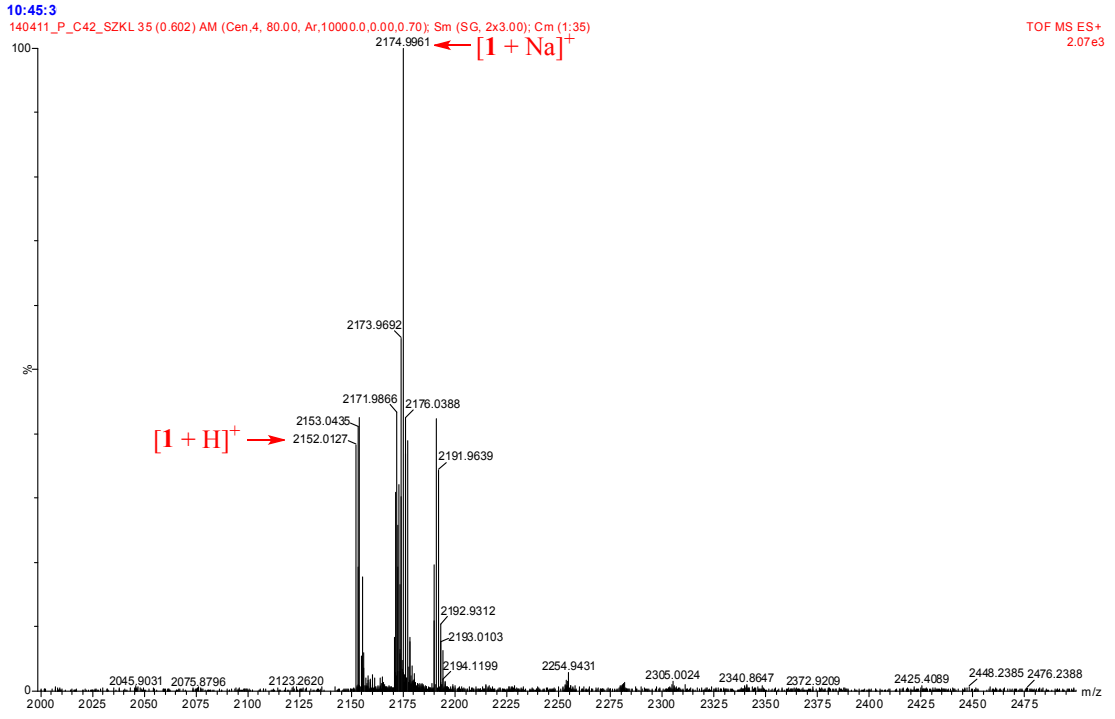

Fig. S11 ESI-HRMS spectrum of **1**.

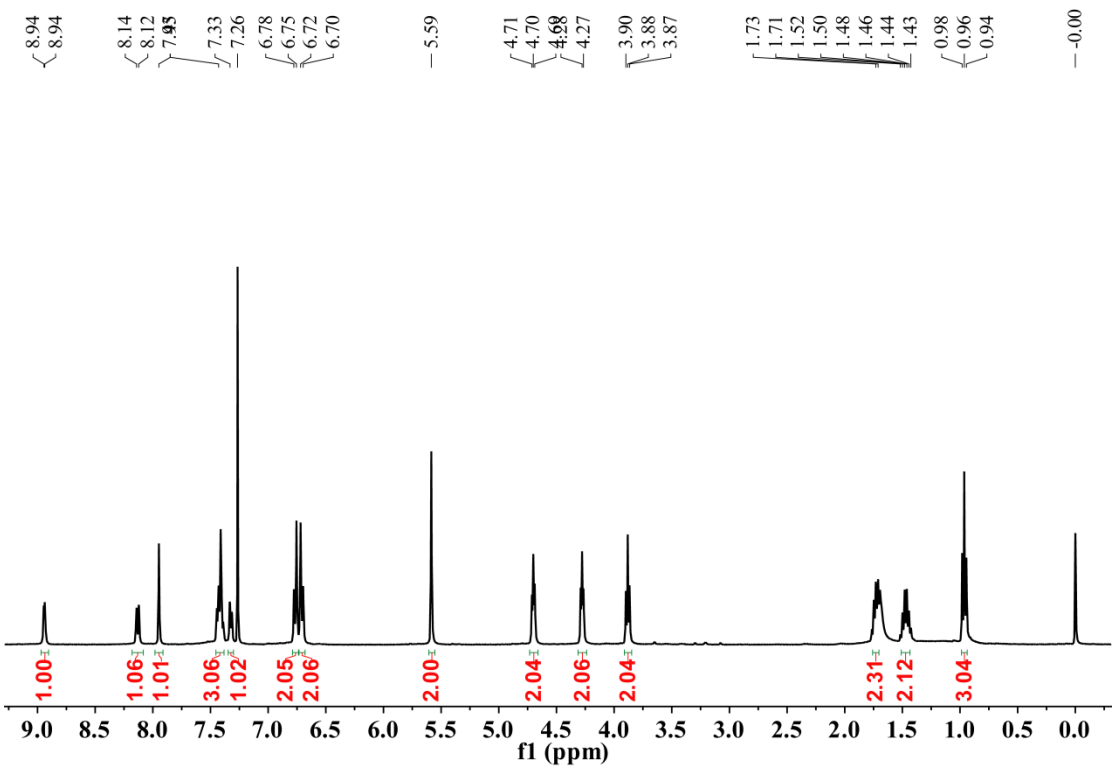

Fig. S12 ^{1}H NMR spectrum (400 MHz, $CDCl_3$) of **2** at 298 K.

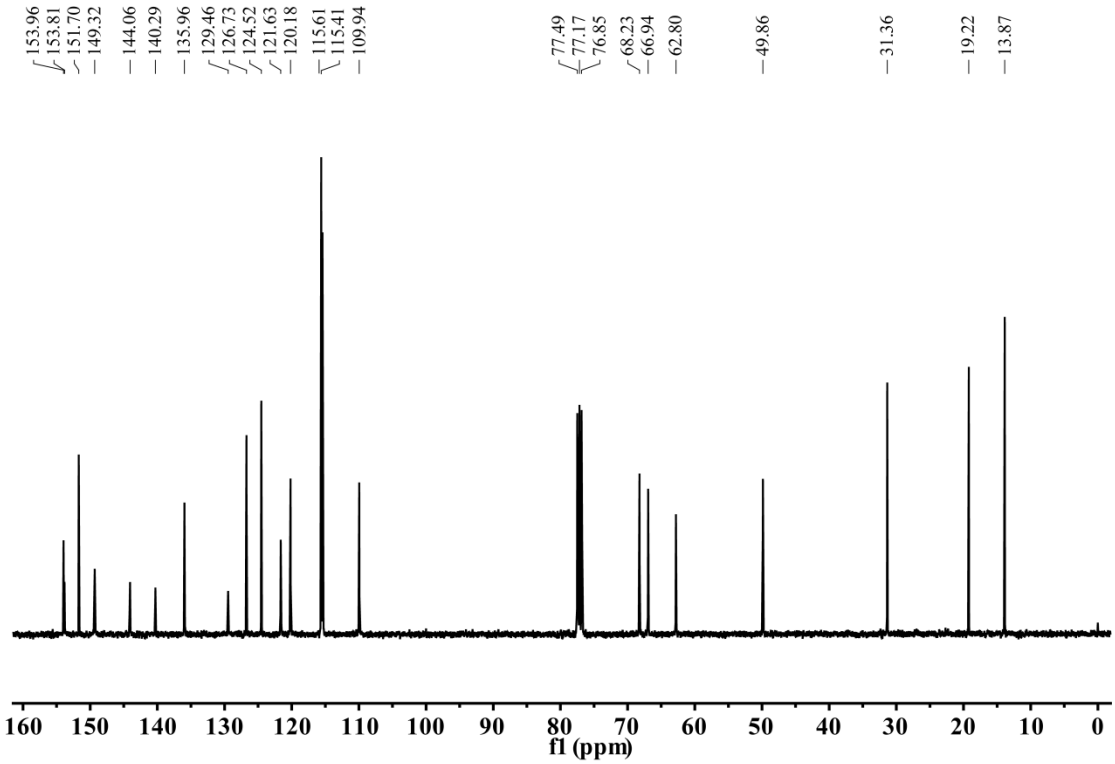

Fig. S13 ^{13}C NMR spectrum (100 MHz, $CDCl_3$) of **2** at 298 K.

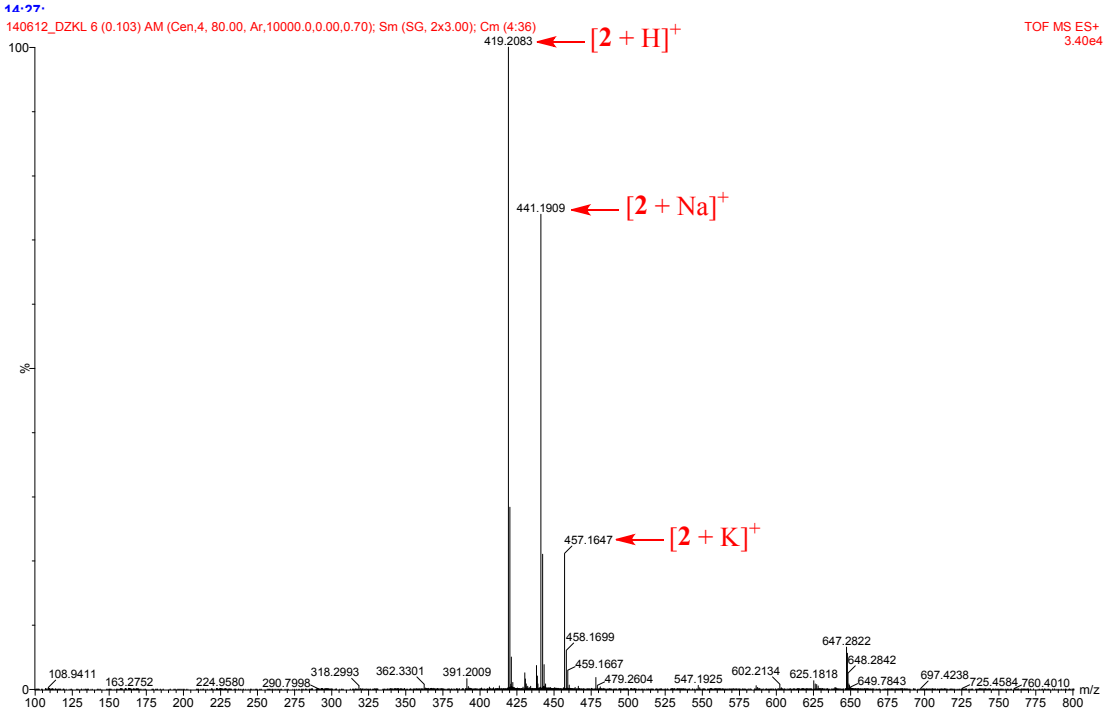

Fig. S14 ESI-HRMS spectrum of **2**.

4. ESI-HRMS for 1-Th^{4+} complex

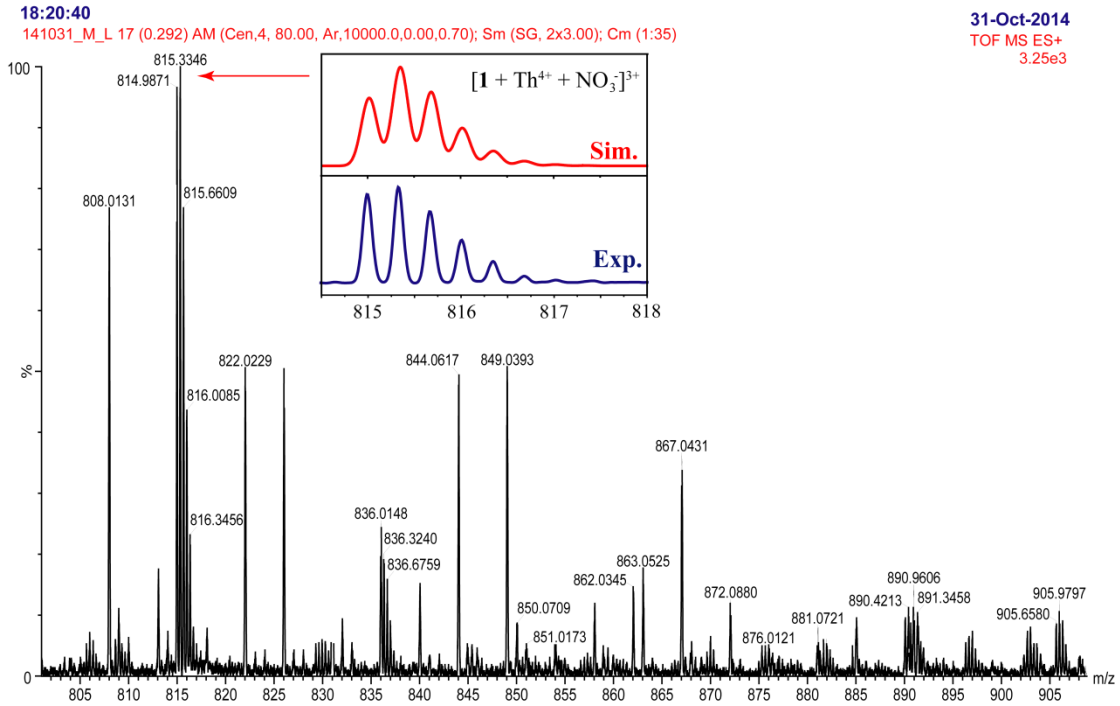

Fig. S15 ESI-HRMS spectrum of the 1:1 (M:L) complex formed between **1** and Th^{4+} (inset: experimental isotope distribution (blue) and computer simulation (red)).

5. ^{1}H NMR spectra of 1 and 1-Th^{4+} complex

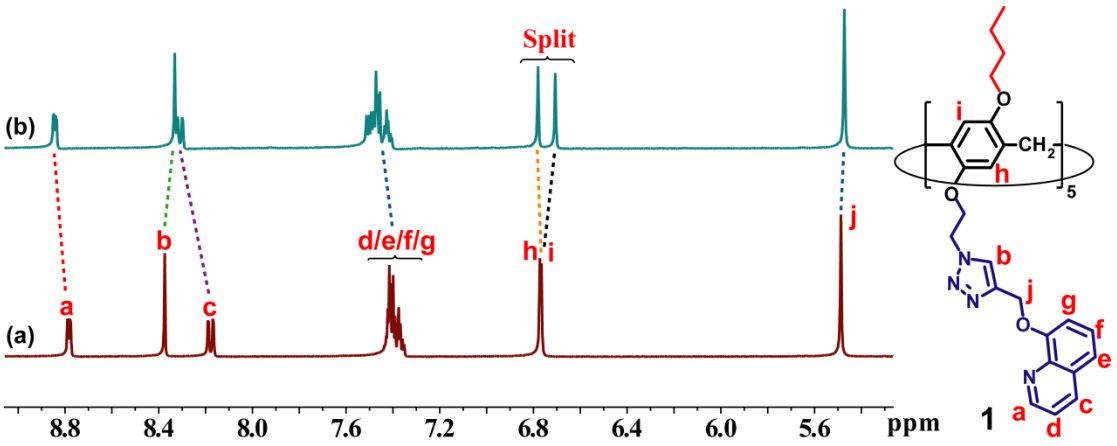

Fig. S16 Stacked partial ^{1}H NMR spectra in acetone-d_6: (a) **1** (2 mM); (b) **1** + Th^{4+} (1:1, 2 mM).

Table S1 Chemical shifts of **1** before and after complextion with Th^{4+} in acetone-d_6.

Proton type	Peak	**1**	**1** + Th^{4+}	Δδ
H_a	m	8.77	8.83	+0.06
H_b	s	8.36	8.32	-0.04
H_c	m	8.16	8.29	+0.13
$H_{d,e,f,g}$	m	7.38	7.44	+0.06
H_h	s	6.76	6.77	+0.01
H_i	s	6.75	6.72	-0.03
H_j	s	5.47	5.46	-0.01

6. Fluorescence and absorption studies

General

The metal ions (La^{3+}, Ce^{3+}, Pr^{3+}, Nd^{3+}, Sm^{3+}, Eu^{3+}, Gd^{3+}, Er^{3+}, Yb^{3+}, Lu^{3+}, Th^{4+},

UO_2^{2+}, Na^+, Ca^{2+}, Cu^{2+}, Zn^{2+}, Pb^{2+} and Cd^{2+}) were used as their nitrates. The anions (F^-, Cl^-, Br^- and I^-) were used as their tetrabutyl ammonium salts. All stock and working solutions were prepared in spectroscopic grade CH_3CN and ultrapure water. The samples of **1** and **2** (1.0×10^{-5} mol•L^{-1}) were freshly prepared in CH_3CN/H_2O (9:1, v/v). The solvent ratio was kept constant throughout the experiment. The fluorescent and UV-Vis spectra were recorded according to the following experiments: 3.0 mL of the solution of compounds **1** and **2** (1.0×10^{-5} mol•L^{-1}) in CH_3CN/H_2O (9:1, v/v) was titrated by adding 10 μL of different metal ions (3.0×10^{-3} mol•L^{-1}) in the same medium. The addition was limited to 100 μL so that the volume change was not significant. The test solution was allowed to stand for 5 min which is long enough to reach the complexing equilibrium before recording the absorption and emission spectra. The excitation was carried out at 310 nm with 5 nm emission slit width in spectrofluorometer.

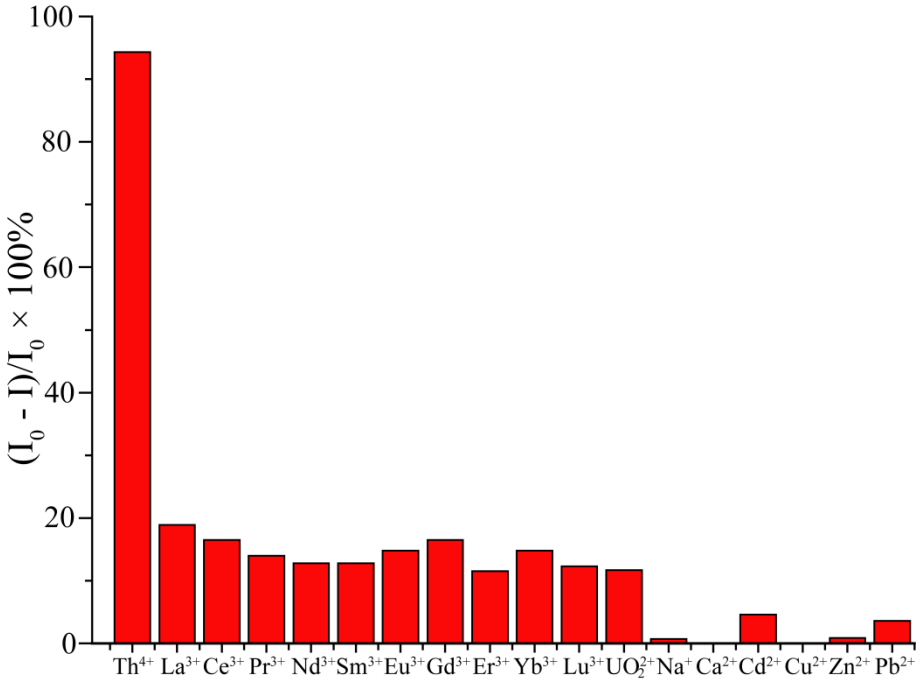

Fig. S17 Fluorescence intensity changes ((I_0-I)/I_0 × 100%) of **1** (10 μM) in a mixed aqueous medium (CH_3CN-H_2O, v/v = 9:1, λ_{ex} = 310 nm) upon addition of 1.0 equiv. of various metal ions. I_0 is the fluorescent emission intensity at 390 nm of each free host and I is the fluorescent intensity after adding metal ions.

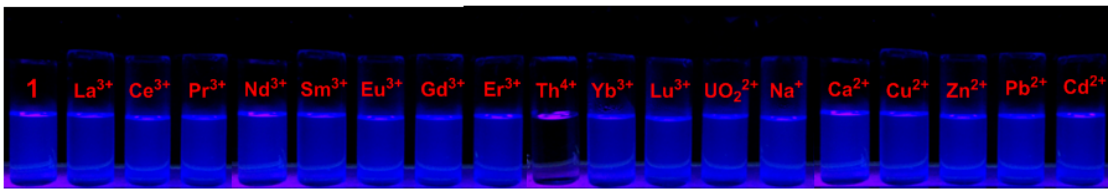

Fig. S18 Visual changes of **1** (50 μM) upon addition of 1.0 equiv. of different metal ions upon excitation at 365 nm using a UV lamp.

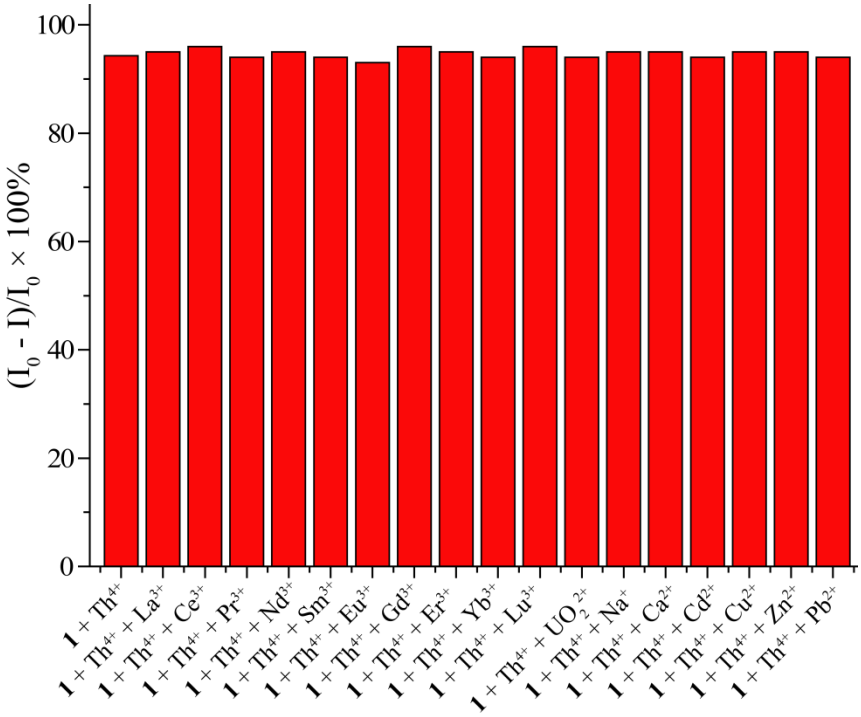

Fig. S19 Fluorescence intensity changes ((I_0-I)/I_0 × 100%) of **1** (10 μM) in a mixed aqueous medium (CH_3CN-H_2O, v/v = 9:1) upon addition of 1.0 equiv. of various metal ions in the presence of 10 equiv. of background metal ions. I_0 is the fluorescent emission intensity at 390 nm of each free host and I is the fluorescent intensity after adding metal ions.

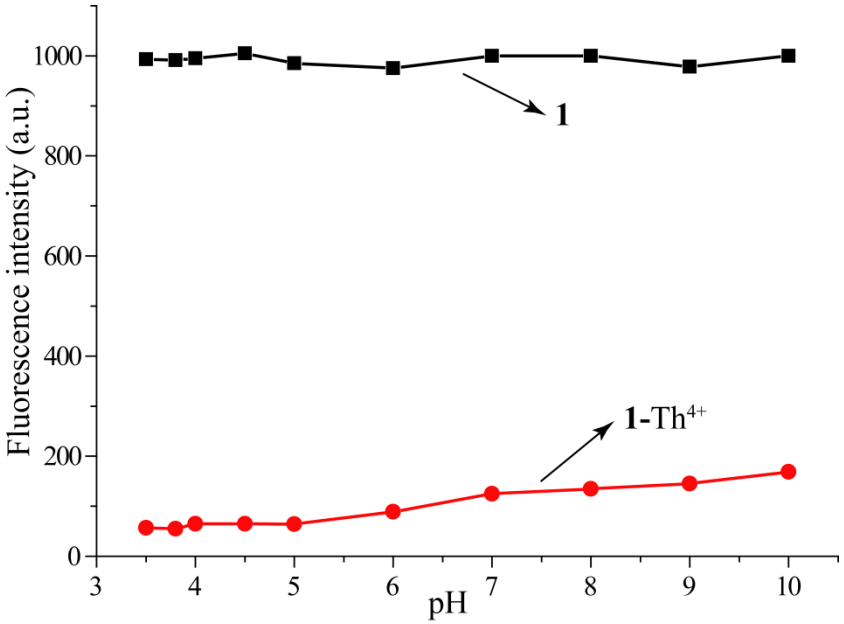

Fig. S20 Plot of fluorescence intensities at 390 nm of **1** (10 μM) and **1**-Th^{4+} ensemble (10 μM) in a mixed aqueous medium (CH_3CN-H_2O, v/v = 9:1; λ_{ex} = 310 nm) versus pH value (using NaOH and HCl to adjust pH to the desired value).

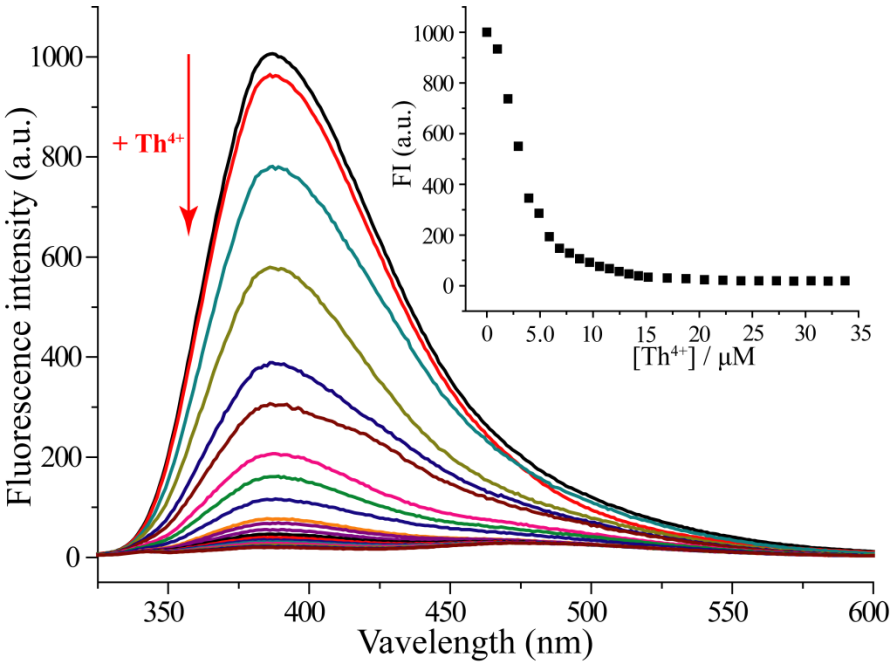

Fig. S21 Fluorescence titration of **1** with Th^{4+} in a mixed aqueous medium (CH_3CN-H_2O, v/v = 9:1; λ_{ex} = 310 nm). Inset: fluorescence intensity at 390 nm as a function of Th^{4+} concentration.

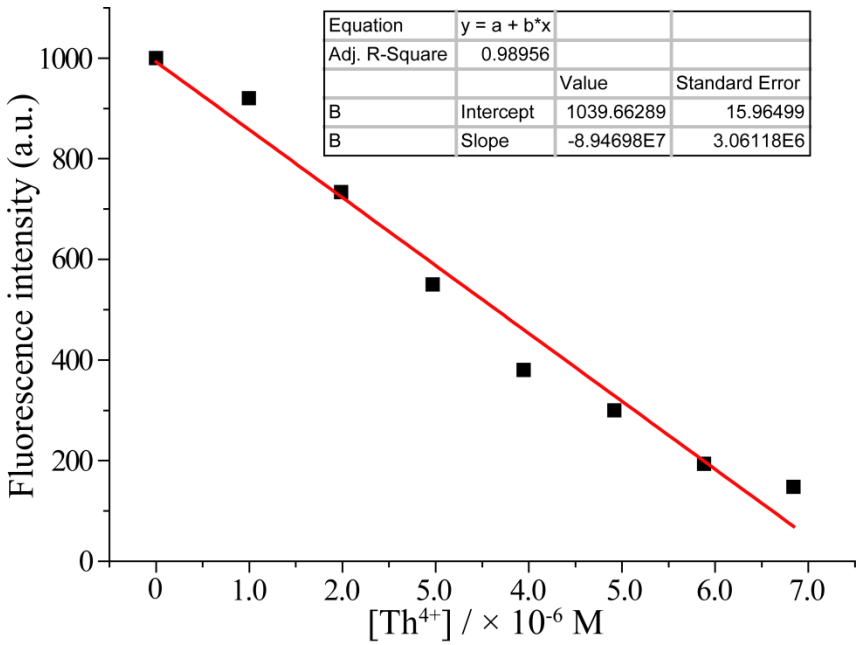

Fig. S22 Curve of fluorescence intensity at 390 nm of **1** (10 μM) in a mixed aqueous medium (CH_3CN-H_2O, v/v = 9:1) versus increasing amount of Th^{4+}.

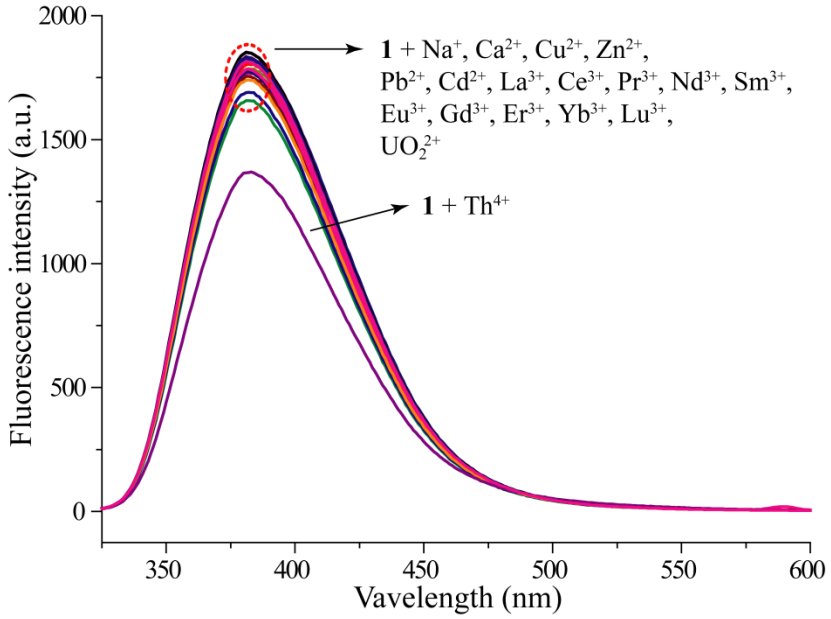

Fig. S23 Fluorescence emission spectra of **2** (50 μM) in the presence of various metal ions (1.0 equiv.) in a mixed aqueous medium (CH_3CN-H_2O, v/v = 9:1; λ_{ex} = 310 nm).

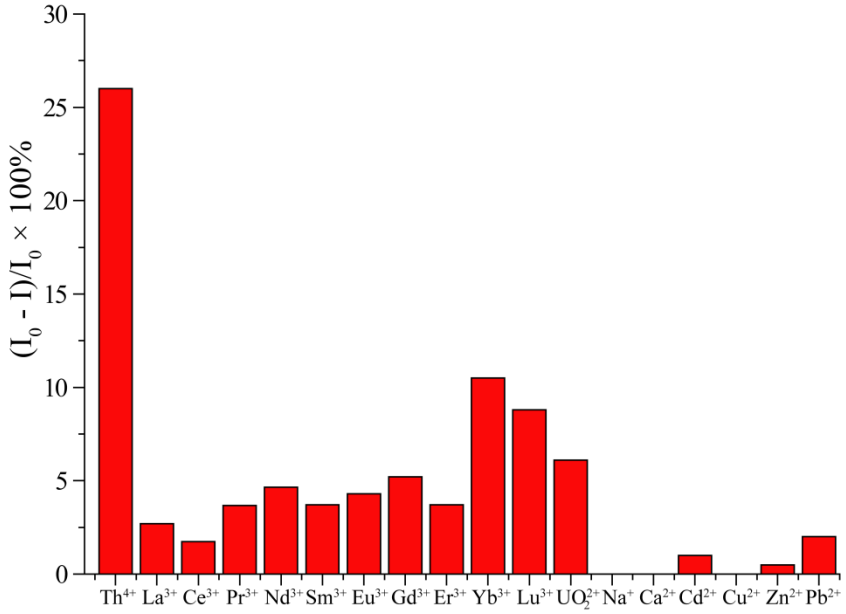

Fig. S24 Fluorescence intensity changes ((I_0-I)/I_0 × 100%) of **2** (50 μM) in a mixed aqueous medium (CH_3CN-H_2O, v/v = 9:1) upon addition of 1.0 equiv. of various metal ions. I_0 is the fluorescent emission intensity at 391 nm of each free host and I is the fluorescent intensity after adding metal ions.

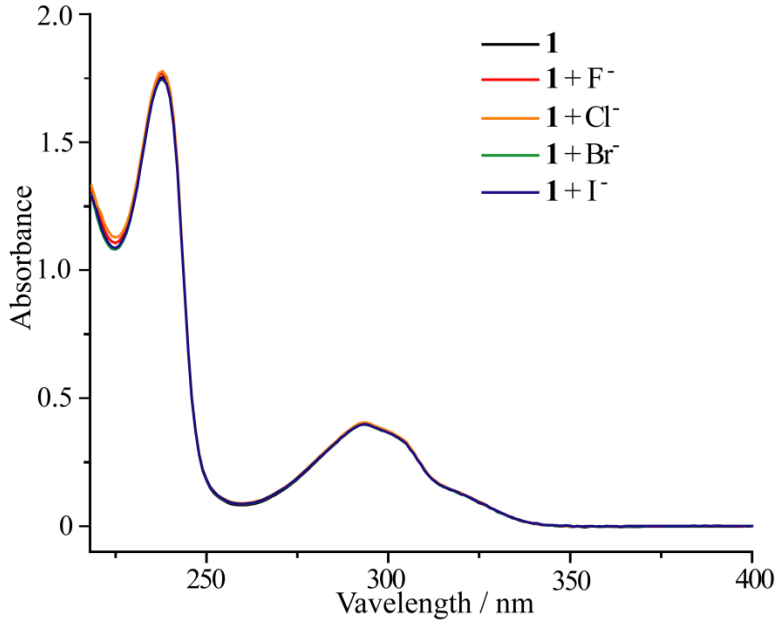

Fig. S25 Absorption spectra of **1** (10 μM) in the presence of different anion species (10 equiv.) in a mixed aqueous medium (CH_3CN-H_2O, v/v = 9:1).

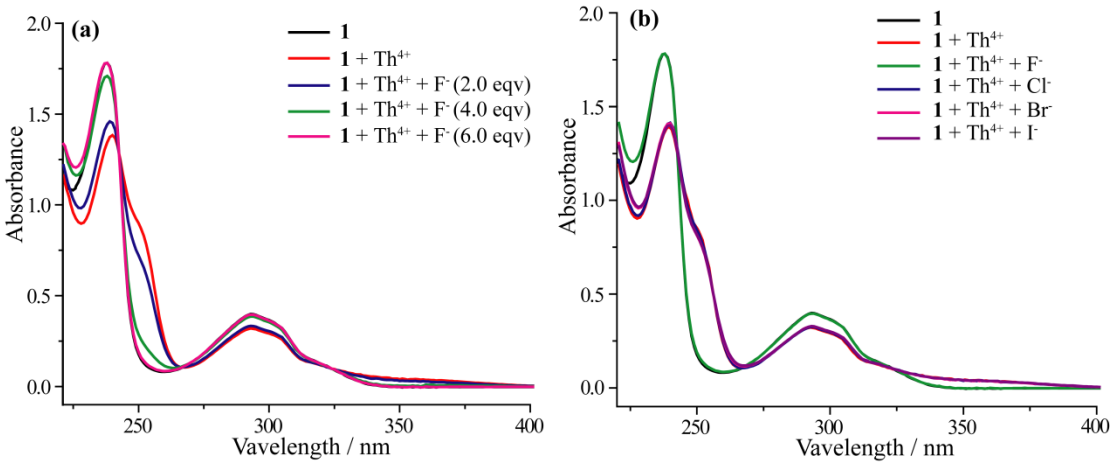

Fig. S26 (a) Absorption spectra of **1** (10 μM) in the presence of Th^{4+} (1.0 equiv.) followed by addition of different equivalent of F^-; (b) Absorption spectra of **1** (10 μM) in the presence of Th^{4+} (1.0 equiv.) followed by addition of different anion species (6.0 equiv.) (solvent: CH_3CN-H_2O, v/v = 9:1).

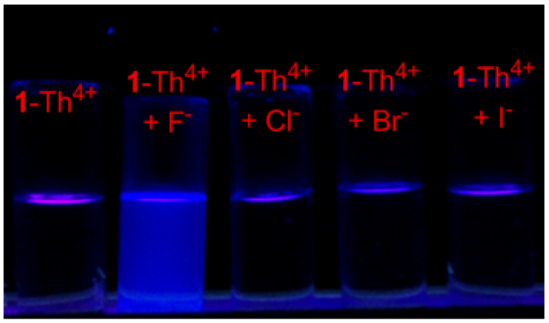

Fig. S27 Visual changes of **1**-Th^{4+} ensemble (50 μM) upon addition of 6.0 equiv. of different halides upon excitation at 365 nm using a UV lamp.

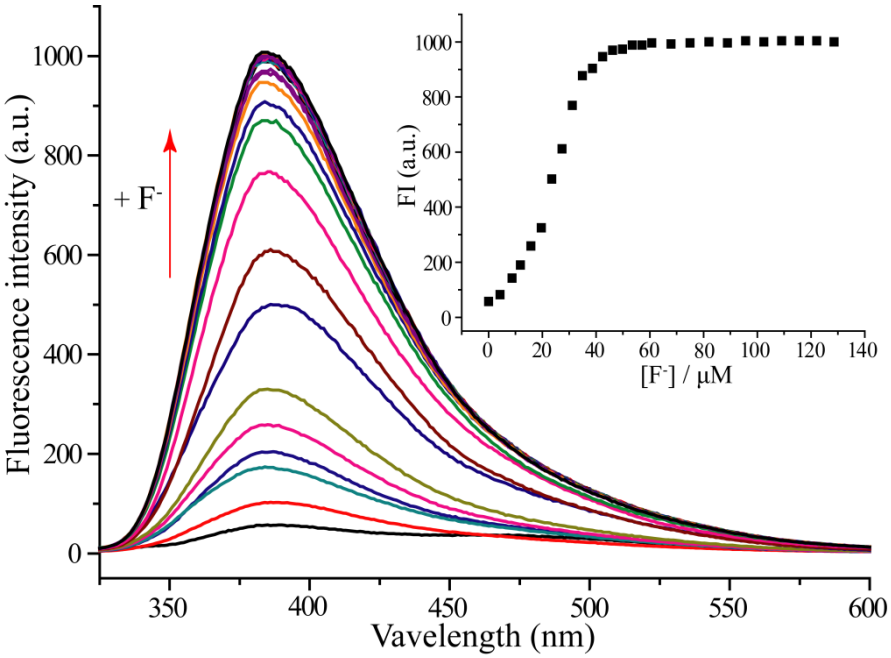

Fig. S28 Fluorescence titration of the **1**-Th^{4+} complex (10 μM) with fluoride ion in a mixed aqueous medium (CH_3CN-H_2O, v/v = 9:1; λ_{ex} = 310 nm). Inset: fluorescence intensity as a function of F^- concentration.

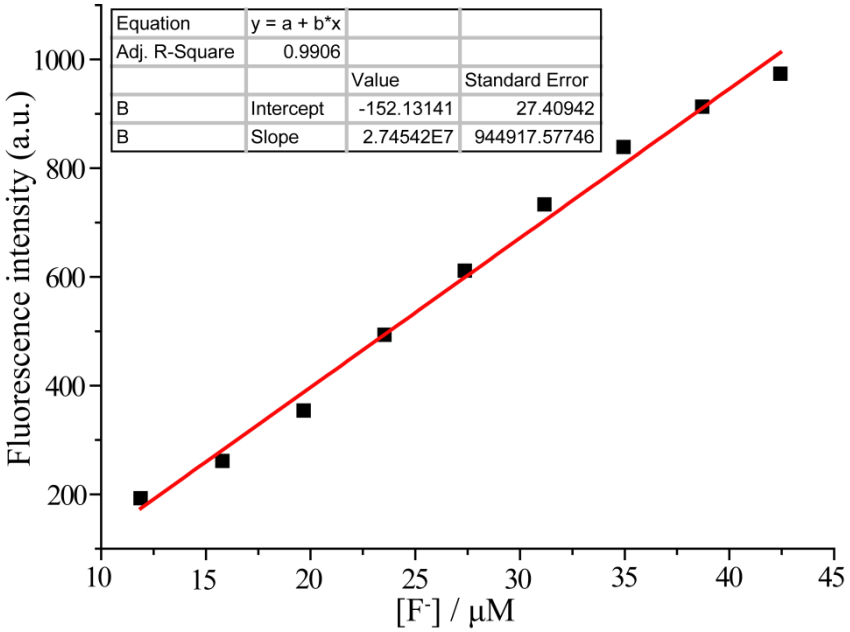

Fig. S29 Curve of fluorescence intensity at 390 nm of **1**-Th^{4+} complex (10 μM) in a mixed aqueous medium (CH_3CN-H_2O, v/v = 9:1) versus increasing amount of F^-.

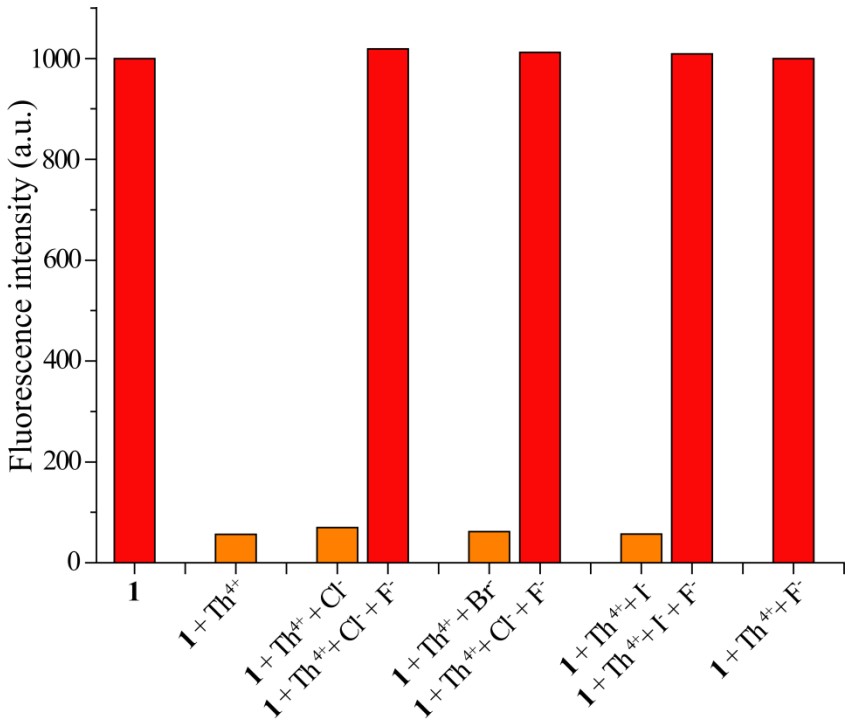

Fig. S30 Fluorescence intensity changes of **1**-Th^{4+} ensemble (10 μM) in the presence of other halides (100 equiv.) followed by addition of F^- (6.0 equiv.) in a mixed aqueous medium (CH_3CN-H_2O, v/v = 9:1, λ_{ex} = 310 nm).

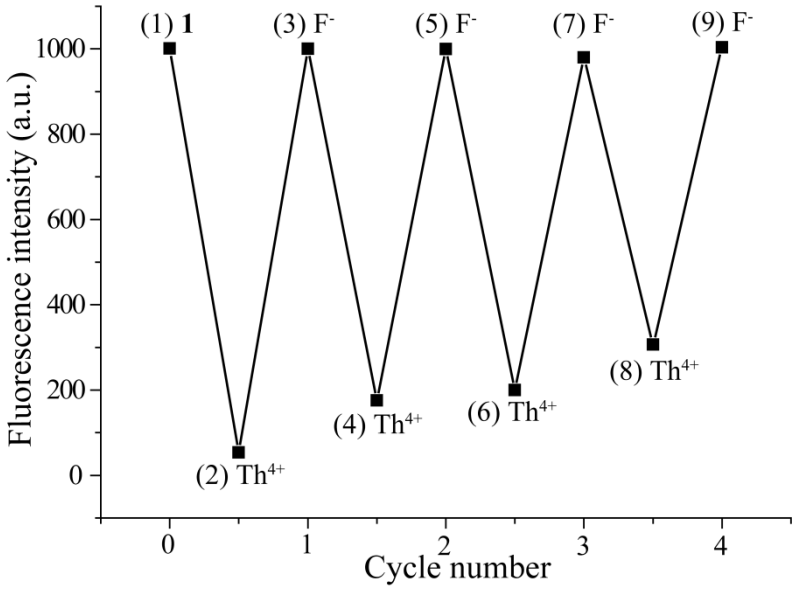

Fig. S31 Fluorescence intensity changes of **1** (10 μM) at 390 nm in a mixed aqueous medium (CH_3CN-H_2O, v/v = 9:1; λ_{ex} = 310 nm) as a function of cycles upon alternate addition of Th^{4+} and F^-, where (1) = **1**; (2) = **1** + Th^{4+}; (3) = (2) + F^-; (4) = (3) + Th^{4+};

(5) = (4) + F^-; (6) = (5) + Th^{4+}; (7) = (6) + F^-; (8) = (7) + Th^{4+}; (9) = (8) + F^- ([Th^{4+}] = 10 μM; [F^-] = 60 μM).

7. References

[S1] L. Weng, J.-J. Yan, H.-L. Xie, G.-Q. Zhong, S.-Q. Zhu, H.-L. Zhang and E.-Q. Chen, *J. Polym. Sci. Part A: Polym. Chem.*, 2013, **51**, 1912-1923.

[S2] Z. Zhang, Y. Luo, B. Xia, C. Han, Y. Yu, X. Chen and F. Huang, *Chem. Commun.*, 2011, **47**, 2417-2419.

[S3] Y.-M. Zhang, Y. Chen, Z.-Q. Li, N. Li and Y. Liu, *Bioorg. Med. Chem.*, 2010, **18**, 1415-1420.